PAPER NUMBER

141

CORROSION 91

The NACE Annual Conference and Corrosion Show

March 11-15, 1991 • Cincinnati Convention Center • Cincinnati, Ohio

CRITICAL ISSUES IN ELECTROCHEMICAL CORROSION MEASUREMENT TECHNIQUES FOR STEEL IN CONCRETE

Alberto A. Sagues
Department of Civil Engineering and Mechanics
University of South Florida
Tampa, Florida 33620

ABSTRACT

Corroding reinforcing steel in concrete presents complicated polarization conditions that make corrosion rate measurement difficult. The polarization response of a mixed-potential electrode is discussed and applied to the case of steel in concrete. Critical issues addressed include the applicability of simple polarization resistance techniques, the effect of excitation current distribution, the effect of diffusional polarization on the cathodic reaction response, interfacial capacitance effects, and the use of guard electrodes.

Key Words: Corrosion, steel, concrete, polarization, corrosion rate, transmission line, impedance, diffusion polarization, guard electrode.

INTRODUCTION

Objective

Corrosion of reinforcing steel in concrete has become a major factor in reducing the service life of vital transportation and building systems. Electrochemical techniques provide virtually the only method of quantitatively assessing the rate of corrosion of steel embedded in concrete in a non-destructive manner. However, the nature of the corroding system presents significant challenges to performing reliable measurements. This paper will highlight some of the problems and critical issues that need to be addressed to develop useful electrochemical test methods in the concrete environment.

The Corrosion Problem

Reinforcing steel is embedded in concrete to provide resistance to tensile stresses. In new, uncontaminated concrete the alkaline environment in contact with the surface of the reinforcing steel causes it to be passive. Metal dissolution proceeds at an exceedingly small rate. However, if local depassivation takes place (for example due to chloride ions reaching the surface of the steel by penetrating through the concrete cover, or if carbonation reduces the pH of the concrete pore liquids), active corrosion may ensue. The corrosion can have conspicuous consequences even if the average rate of metal loss is on the order of a few micrometers per year. This is because corrosion products usually occupy a larger volume than the initial steel, and the surrounding concrete can accommodate very little expansion before cracking. As a result, corrosion-caused cracks and spalls of the concrete cover may happen within a few years of service time. These cracks in turn provide further access to corrosive environmental agents which accelerate degradation of the structure. In recent years this mode of deterioration has threatened the integrity of the transportation infrastructure worldwide, and methods for detection and control have received extensive attention.

The Corroding System

The material surrounding the embedded steel consists of hardened cement paste and of concrete aggregates (stone, sand). The paste and the aggregates are porous, and the pores are often partially filled with a water solution. This solution is rich in K, Na and Ca ions and the pH is typically near 13 [1]. If chloride ions arrive as a contaminant to the surface of the steel, the surface tends to become active when the molar ratio of Cl to hydroxyl ions in the pore solution reaches a critical value, thought to be about 0.3 [2]. Microscopically, the concrete acts as a non-homogeneous electrolyte. Macroscopically, the concrete may be viewed as a medium with an equivalent homogeneous resistivity which varies greatly with the overall moisture content [3,4]. Water-saturated concrete tends to show resistivities on the order of a few Kohm-cm, while oven-dried concrete can approach resistivity values typical of electrical insulators.

In the open circuit potential regimes normally encountered in steel in concrete, oxygen reduction is the most likely corrosion cathodic reaction. Oxygen needs to reach the surface of the steel by transport through the concrete cover. In the absence of cracks, this transport is expected to be by diffusion through the heterogeneous concrete matrix. Tuutti [5] has reported that the diffusion coefficient is dependent on the moisture content of the concrete, with values on the order of 10^{-5} cm^2/sec in water-saturated concrete, and several orders of magnitude higher for concrete stabilized in contact with 50% relative humidity air. However, the general applicability of these results cannot yet be ascertained since few investigations in this area have been reported by others [6,7].

The anodic reaction takes place at the steel surface. In common reinforcing steel bars (rebars) the steel is a pearlitic, hypoeutectoid carbon steel containing about 98% iron. Corrosion may be localized to a few mm^2, or extend over the length of the rebar, which could be many meters. In a structure containing mats of tied-together rebar the steel can be an electrical continuous body extending over hundreds of square meters. The physical cross-section, moisture content and chemical condition (for example chloride content) of the concrete can vary significantly across the rebar assembly. This can generate complex macrocell patterns, which may shift with time depending on weather changes and the type of service encountered by the structure.

Corrosion Measurements

Because the steel is embedded in concrete, non-destructive measurements of corrosion rate must rely in external, indirect estimations of the rate of metal loss. Methods based on dimensional changes [8] and correlation of electrical resistance with loss of steel cross-section [9] have been used. However, the small value of the corrosion rates has encouraged the use of sensitive electrochemical corrosion rate measurements. Unfortunately, the nature of the corroding system presents a sizable challenge to the ability to accurately evaluating the rate of steel deterioration. Measurement and interpretation problems stem from slow transport of chemical species within the concrete, high ohmic resistances, localized corrosion, and the spread of the system over macroscopic distances. These factors make for a slow polarization response to external excitation, so that long test times may be required to assess in detail the electrochemical behavior. At the same time, concrete structures are subject to varying environmental action, disturbing the stability desired in extended tests.

This paper will discuss critical issues encountered at present in attempting non-destructive, electrochemical evaluation of rates of deterioration of steel in concrete. The discussion will focus on excitation/response measurements, with special emphasis on systems where corrosion is due to chloride contamination of the concrete.

ELECTROCHEMICAL METHODS OF CORROSION RATE EVALUATION

Discrete System Approximation

Evaluations of corrosion rates of steel in concrete are often made, on a first approximation, by considering the system as a discrete, mixed potential electrode resulting from the simultaneous reactions:

$$m = m^+ + n_m e \qquad (1)$$

$$x = x^+ + n_x e \qquad (2)$$

where m and m^+ are the reduced and oxidized states of the metal, x and x^+ those of the species that undergoes net reduction in the corrosion process, and n_m , n_x the number of electrons exchanged in each case.

The rate at which the individual oxidation and reaction portions of each reaction take place may be proposed to proceed in direct proportion to the concentration of the appropriate specie at the metal surface, and increasing exponentially with the overpotential (reflecting the chances of overcoming an activation energy barrier). This can be formulated in the manner of Butler-Volmer kinetic equations [10] as:

$$i_{mr} = i_{om} (C_{m+}/C_{m+u}) \exp (2.3 (E_{om} - E)/b_{mc}) \quad (3)$$

$$i_{mo} = i_{om} (C_m/C_{mu}) \exp (2.3 (E-E_{om})/b_{ma}) \quad (4)$$

$$i_{xr} = i_{ox} (C_{x+}/C_{x+u}) \exp (2.3 (E_{ox}-E)/b_{xc}) \quad (5)$$

$$i_{xo} = i_{ox} (C_x/C_{xu}) \exp (2.3 (E-E_{ox})/b_{xa}) \quad (6)$$

where i_{mr}, i_{xr}, i_{mo} and i_{xo} are the current densities for reduction and oxidation, respectively for the species involved, when the potential of the system is E. E_{om} and E_{ox} are the potentials for reactions (1) and (2) respectively at an equilibrium condition when the species have concentrations C_{m+u}, C_{mu}, C_{x+u} and C_{xu}, with i_{om} and i_{ox} as the corresponding exchange current densities. C_m^+, C_m, C_{x+}, and C_x are the actual concentrations of the species at the metal surface when the potential is E. The magnitudes b_{mc}, b_{ma}, b_{xc} and b_{xa} are the activation Tafel constants for the individual partial reactions. As defined here, these are actual activation constants, and not effective or apparent slopes that may change as the polarization state of the system is varied. The nomenclature for these magnitudes is not uniform in the corrosion literature.

At the mixed (corrosion) potential E_{corr}, charge neutrality dictates that

$$i_{mr} + i_{xr} = i_{mo} + i_{xo} \quad (7)$$

If the potential is deviated from E_{corr}, Eq.(7) will no longer be in balance and an externally supplied current will be required to make up for the imbalance. If the externally imposed potential deviation and current are measured, those values can be used in conjunction with equations (3-6) to calculate the corrosion current density i_{corr} (which is the value of i_{mo}-i_{mr} when $E=E_{corr}$). The calculations are simplified if E_{corr} is sufficiently above E_{om} and below E_{ox} to make both i_{mr} and i_{xo} negligible compared with i_{mo} and i_{xr}. This condition tends to be achieved when E_{om} and E_{ox} differ from E_{corr} by an amount equal to several times the magnitude of the corresponding activation Tafel slopes. In that case Eqs. (3-7) can be replaced by

$$i_{mo} = i_{corr} \exp (2.3 E_{dev}/b_a) \quad (8)$$

$$i_{xr} = i_{corr} \exp (-2.3 E_{dev}/b_c) \quad (9)$$

$$i_{ap} = i_{mo} - i_{xr} \quad (10)$$

where E_{dev} is the difference between the applied potential and E_{corr}, i_{ap} is the applied current density, and b_a and b_c are equal to b_{ma} and b_{xc} in Eqs.(3-6). While that assumption may be used on first approximation to facilitate the determination of corrosion rates of steel in concrete, notable complications still remain from the presence of transient electrochemical phenomena due to interfacial capacitance and diffusional transport effects.

The metal-electrolyte interface can store electrical charge much as an electrical capacitor does. The mechanism of charge accumulation is complex, and it may involve electronic surplus or depletion on the metal side of the interface, and reorientation of polar molecules or adsorption of substances on the electrolyte side [11,12]. The amount of charge accumulation is a function of the interfacial potential difference. If an interface undergoes a small potential change dE the corresponding change in the amount of charge (dQ) may be considered to be approximately linearly

proportional to the change in potential. The interfacial capacitance C is then defined by

$$C = dQ/dE \qquad (11)$$

On first approximation, C may be assumed to be independent of the rate of potential change [11]. In that case, the amount of current needed to provide the charge dQ is a simple function of the rate of potential change with time:

$$i_c = dQ/dt = C\, dE/dt \qquad (12)$$

In a corrosion rate measurement, this current must be added to that used to change the potential of the corrosion reactions. Elimination of the capacitive transient current in actual measurements necessitates using very slow potential change rates, or waiting for a time after each change.

Diffusional transport proceeds at a finite rate, which causes the concentration of the electrochemically active species at the metal surface to be different from the unpolarized values (Eqs.(3-6)). At E_{corr} the surface concentrations have achieved certain steady state values. If the system is deviated from E_{corr} the surface concentrations will experience changes from the steady state values. Those changes will be time-dependent and determined by the transport rates pertinent to each species. While the surface concentrations change with time, so will also the polarization state of the system. In the case of a potential deviation this translates into another transient current to be added to the interfacial capacitance effects discussed above. These effects need to be carefully considered when selecting the speed at which measurements are conducted in reinforced concrete.

Small-Signal Polarization Techniques

Corrosion rate measurements are sometimes conducted by imposing significant deviations from Ecorr and determining the value of applied current required. If diffusional transport effects are not important and the potential changes are conducted very slowly, it is possible to determine with reasonable accuracy the relevant parameters in Eq.(8-10). These large-signal tests are typified by the Tafel Extrapolation method, which has been used with success to determine corrosion rates of metals in contact with free liquid electrolytes. However, severe difficulties develop when attempting to apply this method to steel in concrete. If the potential excursion is in the anodic direction, there is danger of irreversibly triggering pitting during the test if an otherwise subcritical chloride concentration is present at the steel surface. If the excursion is conducted instead in the cathodic direction, capacitive and diffusional effects as indicated earlier may be important. As a result, simple Tafel behavior is rarely observed. In addition, the ohmic resistance of concrete is high, and IR-drop becomes difficult to compensate accurately at the relatively high currents created by the wide potential excursion. Because of these factors, Tafel extrapolation has encountered limited use [13] as a means of corrosion rate evaluation for steel in concrete.

Small-signal (that is, potential deviations much less than the magnitude of the Tafel constants) polarization measurements in concrete tend to avoid permanent system upsets and permit more reliable compensation of errors due to high electrolyte resistivity. These methods take advantage of the quasi-linear relationship between applied current and potential deviation that may be encountered when the latter is small. For example, if diffusional effects and transient behavior

can be neglected, Eqs. (8-10) for small values of E_{dev} reduce to [14,15]:

$$E_{dev}/i_{ap} = B/i_{corr} \qquad (13)$$

with $B = b_a b_c/2.3\ (b_a+b_c)$ in this particular case.

This is a form of the Stern-Geary equation, showing that the ratio of potential deviation to applied current is inversely proportional to the corrosion current density (IR drops need to be addressed separately). The ratio E_{dev}/i_{ap} obtained in this case is equal to the Polarization Resistance (R_p) of the system, which is defined as the limit value of E_{dev}/i_{ap} when the potential is varied at an infinitely slow rate, and at the small-signal limit. The proportionality factor B is in the case under consideration a simple function of the activation Tafel constants of the pertinent electrode reactions of the system. Comparable relationships between R_p and $1/i_{corr}$ through a proportionality magnitude B have been developed for other polarization conditions [15]. For example, if the cathodic reaction is under complete diffusional control, Eq.(13) holds but with $B=b_a/2.3$. Approximate values of the activation parameters are often known beforehand from independent measurements, thus providing a value for B if an appropriate relationship exists. Therefore in cases where Eq.(13) is valid and the expression linking B with the activation parameters is known, corrosion rates can be obtained by means of quick and non-destructive measurements. This is the basis for the Polarization Resistance (PR) method of corrosion rate measurement. Sometimes measurements of this type are conducted using somewhat larger potential deviations. The resulting deviation from linearity, if carefully characterized, may provide estimates of the value of the appropriate activation constants, and the small-signal portion of the same experiment is then used to evaluate i_{corr}. In many instances the validity of Eq.(13) cannot be established beforehand. In those cases, polarization resistance measurements have been correlated approximately to corrosion rates determined by mass loss measurements, and the resulting empirical values of B have been used to evaluate corrosion rates in related corrosion systems.

The PR method has been used extensively in attempts to measure corrosion rates of steel in concrete. Good correlation has been shown for laboratory specimens between corrosion rates obtained by PR tests and by independent gravimetric metal loss evaluation [16]. However, that correlation is adequate only within a range of potential scan rates, indicating as expected the important presence of transient phenomena. Other simple small-signal polarization measurements (for example potentiostatic or galvanostatic pulse techniques) present similar questions concerning the effect of transient polarization phenomena.

Corrosion measurement techniques that use quick, simple measurements are highly desirable for steel in concrete, especially in highway applications where road service interruptions have to be kept to a minimum. Evaluation of the errors inherent to the limitations of each test technique is desirable, so that minimum potential scan rates or test times can be established to achieve a desired measurement tolerance. This task is facilitated by the availability of considerable information on the response of corroding systems to small-signal harmonic electrochemical excitation over a wide frequency range, provided by theoretical and experimental Electrochemical Impedance Spectroscopy (EIS) investigations.

Virtually every potential or current variation with time can be approximated by a spectrum of harmonic functions. The response of a corroding system in small-signal test methods such as polarization resistance may then be predicted and analyzed if EIS data are available over a wide enough frequency range. This provides in principle the ability to decide on the appropriate

operation regimes, measurement times, and extrapolation criteria that may be used to evaluate corrosion rates in each measurement technique. Consequently, it is desirable to study the EIS response of steel in concrete as a mixed-potential electrode system. The Faradaic EIS response of a mixed-potential electrode has been addressed in detail by Haruyama [17], using as a starting point Eqs (3-6). If the assumptions are made that E_{corr} is far removed from E_{om} and E_{ox}, and that $C_m = C_{mu}$ (the latter implying unrestricted metal availability at the metal surface), the Faradaic impedance $\mathbf{Z_f}$ of the electrode when species x is under diffusional transport limitation is predicted to be [18,19]:

$$\mathbf{Z_f} = 1/(1/\mathbf{Z_a} + 1/\mathbf{Z_c}) \tag{14}$$

with

$$\mathbf{Z_a} = b_a/2.3\, i_{corr} = R_a \tag{15}$$

and

$$\mathbf{Zc} = b_c/2.3\, i_{corr} + [b_c/2.3\, (i_l - i_{corr})] \tanh (\sqrt{ju})/\sqrt{ju} = R_c + W_c \tag{16}$$

where:

R_a, R_c and W_c are as defined in the equations.

i_l = limiting cathodic current density

$u = \omega\, d^2/D$

with $\omega = 2\pi f$
f = frequency of the excitation signal
d = diffusion distance of species x^+
($C_{x+} = C_{x+u}$ at distances from the metal greater than d)
D = diffusion coefficient of species x^+ in the electrolyte

The expression for $\mathbf{Z_f}$ (Eq. 14) was derived analytically from the problem statement [18, 19], without using an electrical circuit analog as the starting point. However, the result has been arranged to show that $\mathbf{Z_f}$ may be viewed as the impedance that would result from the parallel combination of impedances $\mathbf{Z_a}$ and $\mathbf{Z_c}$. $\mathbf{Z_a}$ is a real magnitude, and as such it may be considered as the impedance of a purely resistive component, R_a. Since $\mathbf{Z_a}$ includes only parameters for the anodic reaction, it will be called the anodic branch of the Faradaic impedance. For the same reason, $\mathbf{Z_c}$ will be called the cathodic branch. The first term of $\mathbf{Z_c}$, like $\mathbf{Z_a}$, is real and includes only activation parameters. This resistive term is designated R_c in Eq.(16). The second term in $\mathbf{Z_c}$ is complex and has the form of a finite-distance Warburg impedance, clearly associated with the diffusion process of the cathodic species [20]. This term is designated W_c in Eq.(16).

If interfacial charge accumulation phenomena are assumed to cause the small-signal behavior described in Eq. (12), then the ac current flowing across the corroding interface will be increased by an amount equal to that which would result from placing a capacitor C between the electrolyte and the metal. The electrode used to sense potential changes in corrosion rate measurements needs to be placed at a finite distance from the interface. The intervening electrolyte gap may on first approximation be considered to be equivalent to a purely ohmic resistor R_s. The potential measured will be augmented by the corresponding ohmic potential drop IR_s.

The preceding assumptions and results can be used to formulate an electrical circuit that has an impedance response similar to that of the corroding interface under small signal conditions. This equivalent circuit is shown in Figure 1, and will be used to assess the requirements of measuring techniques to determine the corrosion rate of steel in concrete.

If b_a and b_c were known and both cathodic and anodic action were uniformly distributed over a small system, the corrosion current density could be obtained from EIS measurements performed at various frequencies and subsequent application of the equivalent circuit in Figure 1. The high-frequency limit of the impedance provides the value of R_s. At very high frequencies, the impedance response is dominated by the series combination of the electrolyte resistance (already determined) and the impedance of the capacitor, $-j\,\omega^{-1}C^{-1}$, so that measurements in that regime would yield C. At high frequencies the diffusional component of Z_c is small compared with R_c, so that the impedance response is dominated by the parallel combination of R_a and R_c (designated in the following as $R_a//R_c$), coupled to C and R_s which are already known. The low-frequency limit of this intermediate-frequency response may be used, in cases where C is not very large, to evaluate $R_a//R_c$ as shown in Figure 2 [17]. If C is large, the experimental data from measurements conducted at several frequencies could in principle be used to set up a system of equations to determine $R_a//R_c$.

The magnitude $R_a//R_c$ provides the corrosion current density, since examination of Eqs. (15) and (16) shows that $i_{corr} = b_a b_c/2.3\ (b_a+b_c)(R_a//R_c)$. Notice that $R_a//R_c$ is the same as the polarization resistance (after correcting for R_s) in the case of Eq. (13), which corresponded to a system where diffusional effects and transient behavior could be neglected. When those effects cannot be ignored, Figure 2 shows that the polarization resistance (which is effectively the same as the low-frequency limit of the impedance) can range anywhere from $R_s+(R_a//R_c)$ to R_s+R_a. The latter case corresponds to the extreme of complete cathodic diffusional control ($i_{corr}=i_l$) which causes W_c and hence Z_c to be infinite. That condition does not lead to an infinite value of Z_t, since the anodic reaction still has a finite and real impedance R_a which shunts Z_c. Instead, the low frequency limit of the impedance is simply R_s+R_a. More details on this behavior are encountered in Refs.[17-19] and [21]. Since $R_a=b_a/2.3\ i_{corr}$, this limit agrees with the value of B for the corresponding PR case discussed earlier.

The preceding discussion confirms that after accounting for R_s, the factor B for calculating I_{corr} from polarization resistance measurements is $b_a b_c/2.3(b_a+b_c)$ if there is no diffusional limitation to the cathodic reaction, and $b_a/2.3$ if there is complete diffusional limitation. B will have values in between for partial diffusional control cases. There is no simple relationship between B and the polarization parameters for those intermediate cases [21].

Implications on the Use of Polarization Resistance to Measure Corrosion Rates of Steel in Concrete

This section will address issues present in the use of LP to measure corrosion of steel in concrete in a discrete, uniform system. Further complications arising from localization of corrosion and uneven current distribution are addressed in the following sections.

As shown in the previous section, PR measurements of a discrete, uniform system could provide reasonable estimates of the corrosion rate (when R_s is accounted for), if one knows whether diffusional control is either non-existent or complete, and if the rate of potential variation is low enough to correspond to the low-frequency limit condition. Previous knowledge of the activation parameters b_a and b_c (or approximations thereof) is also required. These requirements pose different levels of difficulty in achieving useful results.

R_s may be measured independently, or its effect may be eliminated in a PR test by measuring potentials in the instant-off current condition. For a discrete system this is relatively straightforward. The extent of the diffusional polarization is generally not known beforehand. However, an estimate of the possible errors involved can be made by considering the Tafel slope values likely to be encountered. For the anodic reaction b_a is expected to be on the order of 60 mV, while the Tafel slope for oxygen reduction on steel in alkaline media is on the order of 160 mV [22]. Therefore, the B constant for use in a PR test would be about 20 mV for the purely activation-controlled case, and about 26 mV for the case of complete diffusional control of the cathodic reaction. As indicated earlier, the case of mixed activation-diffusion polarization control of the cathodic reaction would yield a B value somewhere in between the two other magnitudes. Therefore, in the above example incomplete knowledge of the polarization condition of the cathodic reaction (in a discrete system) would create errors of about 30% or less in the estimated corrosion rate. This error magnitude may be considered to be relatively small, in view the present state of development of corrosion measurement techniques for steel in concrete.

The approximation to the low-frequency limit presents perhaps a more serious difficulty. The results of the measurements will be subject to different errors depending on the schedule used to deviate the potential from Ecorr, and at what moment the current i_{ap} is measured. Corrosion current densities for active steel in concrete range typically from a fraction of 1 uA/cm^2 to over 100 uA/cm^2 [23,24]. For the purpose of early corrosion detection, values of 1 uA/cm^2 or less are of particular interest. This corresponds roughly to polarization resistances on the order of 20,000 ohm.cm^2 or more. In a typical polarization resistance test the maximum voltage deviation is about 10 mV, therefore resulting in typical maximum Faradaic polarization currents on the order of 0.5 uA/cm^2 or less. If a constant potential-time ramp dE/dt is used, then i_{ap} will be affected by an error $i_c = C\, dE/dt$ (as per Eq.(12). For a typical potential scan rate of 6 mv/min, and an interfacial capacitance of 100 uF/cm^2 (see below) i_c is expected to be on the order of 0.01 uA/cm^2 or higher. If the actual value of i_{corr} is approximately 1 uA/cm^2, this means that at the highest potential swing i_{corr} will be overestimated by only about 2% (disregarding R_s). However, at the same scan rate the measurement will overestimate i_{corr} by about 200% if i_{corr} is 0.1 uA/cm^2 and C=1000 uF/cm^2.

Various potential-current measurement schedules may be used to minimize error in evaluating Rp [24,25]. In a constant potential ramp test with small R_s the contribution of i_c is roughly constant, and it would result primarily in an offset of the polarization line. The E_{dev}/i_{ap}

slope would closely approach R_p. Accounting for the current offset by instrumentation or data manipulation techniques can reduce considerably the error in the calculated value of R_p. More accuracy in evaluating R_p can be obtained by performing cyclic PR measurements, where a continuous triangular wave is used as the excitation signal. This results in a potential-current diagram resembling a hysteresis loop. The slope of the sides of the loop tends to R_p as the scan rate of the triangular wave approaches zero [26-29]. This permits accurate calculation of R_p by extrapolation from tests performed at various scan rates. The manner in which the potential deviations from E_{corr} are achieved can be important if simple, stepwise variation in conditions are used in an attempt to evaluate R_p. Gonzalez et al [30,31] have shown that under those circumstances the time constant for decay of capacitive currents is R_sC if the step is applied potentiostatically, but it is R_pC if the step is applied galvanostatically. Thus for systems where the concrete resistance is small compared to the polarization resistance (for example, slowly corroding rebar in moist concrete), step measurements should be performed potentiostatically to minimize test time. However, as it will be shown below, the distribution of excitation current over macroscopic distances can slow down the system response and require measurements that take into account the time-dependent behavior.

Knowledge of the activation parameters b_a and b_c is limited and almost always approximate estimates or empirical correlations are used to estimate corrosion rates of steel in concrete. Nevertheless, these parameters have been observed to remain within a relatively restricted range for a variety of corroding systems [15], and the use of approximate values may not cause as much error as some of the other factors considered here. Because of the large transient effects normally observed in steel in concrete, determination of activation parameters with a PR test using larger potential excursions is subject to considerable interpretation difficulties. Detailed experiments of the EIS response of steel in concrete may be necessary to provide better estimates of the activation parameters.

The effect of current distribution.

The discussion above addressed conditions required to obtain useful corrosion rate estimates in a discrete system displaying some of the characteristics of reinforcing steel in concrete. Unfortunately, actual structures do not behave as a discrete mixed potential electrode. The combination of relatively high electrolyte resistivity with macroscopic component sizes causes complicated current distribution patterns to develop. The response of the system to an electrochemical excitation is then the sum of numerous responses from individual surface elements, each with a different polarization condition and excited differently by the test signal.

Evidence of this complication is observed in wide-spectrum polarization measurements, such as in the EIS test results shown in Figure 3 [32,33]. The Nyquist diagram in figure 3A resembles a single semicircle, as it would be expected from the medium-to-high frequency behavior predicted in Figure 2. However, there is considerable distortion at the high frequency end, where the diagram meets the real axis at an angle approaching 45°. Results from testing a different specimen are shown in Figure 3B. There the high frequency distortion is also present, but in addition the diagram shows no indication of converging toward a real value at the low frequency limit.

The high frequency distortion may be explained as being the result of the combination of high concrete resistivity, macroscopic specimen sizes, and the presence of appreciable interfacial capacitance (steel surface roughness and corrosion products may also play an important role, as discussed later). The impedance response of a long concrete beam containing a longitudinal rebar

will be considered as an illustration. As shown schematically in Figure 4, the portions of the bar closer to the excitation point receive a large fraction of the excitation current than those bar portions further away. A simplified model of that situation is presented in Figure 5, where the beam has been divided into longitudinal elements of length dx. Each element has an admittance $dY = Y_l\, dx$, where Y_l is the admittance per unit length. The corresponding element impedance is $dZ = 1/dY$; the magnitude Z_l can be defined so that $dZ = Z_l/dx$. Each element has also a longitudinal resistance $dR = R_l dx$, where R_l is the resistance per unit length which is a function of the concrete resistivity and the beam cross-section. This equivalent circuit has the characteristics of an electric transmission line, and has been used to model a variety of electrochemical systems [34-36]. If the beam has a length L, and if both Z_l and R_l are constant along the beam, the overall impedance Z_t measured from one of the ends is given by the de Levie relationship [36,37]:

$$Z_t = (R_l Z_l)^{1/2} / \tanh (L (R_l/Z_l)^{1/2}) \qquad (17)$$

which, if L is large becomes simply:

$$Z_t = (R_l Z_l)^{1/2} \qquad (18)$$

Figure 6 shows schematically the impedance diagrams expected from Eqs. (17-18) for systems with no corrosion (Z_l corresponding only to interfacial capacitance) and undergoing corrosion (Z_l assumed to correspond to a parallel combination of interfacial capacitance and polarization resistance [36]). The distributed impedance of the interfacial capacitance causes the phase angle of the measured impedance to be close to 45° at the high frequencies. This is a likely cause of the high-frequency semicircle distortion exemplified in Figure 3A and 3B. The low-frequency limit behavior of Z_t is related to the low-frequency limit of Z_l by Eqs.(17-18). Figure 6 shows the low frequency limit value of Z_t for a simple case where Z_l is the parallel combination of a distributed polarization resistance R_{pl} and a distributed interfacial capacitance C_l. The data in Figure 3A might be viewed as corresponding to that case. Experimental determination of the low-frequency limit of Z_t, together with knowledge of R_l would thus permit obtaining R_{pl}, and from there determining the corrosion current per unit bar length by application of Eq. (13).

Methods based on the above approximation were presented by Feliu et al [38-40] to calculate the uniform distributed polarization resistance for reinforced concrete beams and slabs. One- and two-dimensional transmission line configurations were assumed for the beam and slab cases respectively. Potentiostatic step excitation, as in PR measurements, was considered by those investigators to provide enough approximation to the low-frequency limit to ignore reactive impedance effects.

There are instances, however, when extended reinforced concrete systems display significant reactive impedance behavior even at very low test frequencies (as in Figure 3B), making it difficult to estimate the low-frequency limit behavior within reasonable test times. The impedance elements may be more complicated than parallel R C combinations, including for example diffusional terms. The corrosion and resistivity distribution along an extended reinforced concrete structure is likely to be non-uniform. These factors convolute the impedance response of the system, and limit the straightforward use of single point potential-deviation/impressed current measurements (as in simple PR) for corrosion rate evaluation.

In principle, one can set up a model of the corroding system with multiple metal surface

impedance and concrete resistance elements. Accurate impedance measurements at a sufficient number of different test frequencies may provide enough information to write a system of equations for calculating the values of each individual impedance element. Calculations of this type have been presented for simplified systems by Macdonald and coworkers [34,41]. Other investigators have considered the convolution of the overall impedance response based on the behavior of individual elements [32,42-44]. Attempts are being made at present to establish the applicability of this approach to actual highway bridge structures [44]. The ability of these procedures to provide consistent and unambiguous results needs to be evaluated.

Diffusional polarization versus transmission line behavior.

The complexity of reinforced concrete systems poses nevertheless a significant challenge to developing a comprehensive polarization model for corrosion rate determination. The nature of the impedance at surface elements of steel in concrete is not satisfactorily known at present. This limits the ability of formulating credible impedance deconvolution models. A special difficulty arises from the similitude of the impedance response of diffusionally limited processes with that of distributed interfacial capacitance in a resistive electrolyte. Both circumstances give rise to an impedance magnitude proportional to the inverse square root of the test frequency, and a phase angle of 45° (Eqs.(16) and (17-18)). This similitude creates ambiguities when attempting to identify polarization mechanisms.

On first consideration, diffusional impedance behavior should not be easily observable. This is because diffusional limitation is most likely to take place only for the cathodic reaction, as in the model in Figure 1. At low frequencies the impedance behavior is dominated by R_a, preventing the observation of a Warburg "tail" in the impedance diagram. At high frequencies the Warburg term has a low impedance, but the activation component of Z_c (which is the value R_c) is finite and of the same order as R_a. Therefore, at high frequencies the Faradaic impedance approaches $R_a//R_c$ and the diffusional term is again overshadowed. This argument would suggest that reactive behavior at low frequencies (as in Figure 3b) is likely due to transmission-line effects. However, impedance diagrams with high angle low frequency components have been observed also in short specimens with relatively high conductivity concrete [29,42,45]. A possible explanation for this issue may be provided by considering that cathodic and anodic regions may be macroscopically separated and occupy significantly different amounts of surface area on the rebar. In the case of a large system, the current excitation may be provided in a predominantly cathodic region, with only a small part of the excitation reaching an anode further away. The overall response would thus reflect the polarization characteristics of the cathode, at least over much of the frequency range sampled.

In the case of a small specimen, disparity in the area of cathodic and anodic regions on the corroding rebar might also result in the observation of an impedance spectrum dominated by a diffusional component. Small anodes coupled to much larger cathodic regions may be present, for example, at the beginning of active corrosion, when the chloride threshold has been exceeded only at isolated spots of the metal surface. Under those circumstances the ac current exciting the anode must concentrate in a relatively small region, resulting in an effectively large electrolyte resistance. For instance, in a flat circular anode of radius r surrounded by a high impedance surface, the effective electrolyte resistance associated with the anode is on the order of $R = \rho / 4r$ [46], where ρ is the concrete resistivity. Thus an isolated anodic spot, 2 mm in diameter in 10,000 ohm-cm concrete would have at low frequencies an equivalent electrolyte resistance of 25,000 ohm. The matching cathodic region, much larger in size, would have an associated solution resistance perhaps orders of magnitude smaller than that of the anode. This concept can be approximated by the

simplified equivalent circuit shown in Figure 7. R_{sa} and R_{sc} represent the electrolyte resistance associated with the anode and cathode respectively; both values can be considerable since reference electrodes in concrete tests are usually not placed immediately next to the rebar but instead near the surface of the concrete. Frequency dependence of R_{sa} and R_{sc} [46] is not considered. Figure 8 shows impedance diagrams calculated using the circuit in Figure 7, by assuming a set of roughly representative polarization parameters. One of the plots qualitatively reproduces the low-frequency behavior shown in Figure 3B. The plots illustrate the variety of EIS responses that may be encountered in systems with virtually the same corrosion rate but with different degrees of diffusional control in the cathodic response. Calculations of this type underscore the difficulty inherent to the problem of evaluating corrosion rate from polarization measurements in concrete.

The interfacial capacitance

The interfacial capacitance of steel in concrete plays a critical role in determining how far away from the excitation point the polarization signal will be felt, for a given test frequency or test duration. As indicated earlier, the interfacial capacitance is also directly related to time-dependent errors in simple polarization measurements. Unfortunately, there is little accurate information available at this time on the actual value of this parameter, or on how it is affected by the material and service conditions encountered. Very smooth, clean metal surfaces are expected to have interfacial capacitances on the order of 20 uF/cm^2 [11]. Mechanical roughening of the surface increases the area of contact between metal and electrolyte, thereby increasing the value of the interfacial capacitance several-fold [47,48]. EIS evaluation of interfacial capacitance of sandblasted passive steel in concrete have yielded values on the order of 100 uF/cm^2 [32]. Passive rebar with mill scale has shown values one order of magnitude higher [49]. Even higher values have been reported for corroding rebar in concrete [44], suggesting the possibility that semiconductive corrosion products contribute additional finely dispersed surface to the system [50]. Measurement of interfacial capacitance of steel in concrete are complicated by macroscopic current distribution effects of the type mentioned earlier, plus microscopic transmission line phenomena due to the resistance of the electrolyte filling the roughness at the metal surface [36]. These phenomena may cause the impedance of steel in concrete at high frequencies to have a phase angle which is approximately constant but less than 90°. This constant-phase-angle (CPA) behavior, illustrated in Figure 9 causes uncertainty in the measured value of the interfacial capacitance C, which is often evaluated by assuming that at high frequencies $Im(Z) = 1/\omega C$.

Current confinement ("guard") electrodes.

Corrosion measurement uncertainties due to current distribution effects could be minimized if the excitation current were to be limited to a region of known dimensions in an otherwise extended reinforced concrete structure. Additional electrodes, typically in the form of a guard ring around the counter electrode, have been used for that purpose. The guard electrode is polarized at the same potential as the counter electrode, but connected to an independent signal source. If the guard electrode is large enough and if the impedance at the metal surface and electrolyte resistance are uniformly distributed, then the counter electrode current will flow only to the portion of the metal surface directly underneath the counter electrode [51-53]. If those conditions are met, the impedance (or other polarization type) measurement will correspond only to a well-defined area, and accurate charge transfer rate measurements could be achieved. Unfortunately, uniform corroding conditions are rarely the case in extended concrete systems, and the excitation current of the area below the counter electrode may differ markedly from that supplied by the counter electrode. Of special interest is the case of a relatively small corroding spot surrounded by a large

passive steel region. At high test frequencies the impedance of the interface is expected to be primarily capacitive and relatively uniform; current distribution should be properly controlled by the guard electrode. At low test frequencies the excitation current may be preferentially directed to the corroding spot, even if it lays somewhat outside the area immediately below the counter electrode. Calculations of current distribution under these cases, and of the errors that may be involved, have been presented in the literature for non-reactive approximations of the interfacial impedance [51,52]. Analysis of the situation considering reactive impedance conditions, coupled with more accurate knowledge of the interfacial capacitance values is needed to ascertain the limits of applicability of this approach. Evaluation of the effectiveness of guard ring electrodes to improve corrosion rate measurement accuracy under practical conditions are now in progress [54], but no definitive results are available as yet.

Additional Issues

The items reviewed in the previous sections are a selection of major issues in the way of reliable measurements of corrosion in concrete. Important concerns not addressed in this paper include the role of corrosion products on the electrochemical response of the system to external excitation, the effect of potential drops at concrete layers near the steel surface or at the outer concrete surface, the electrical inhomogeneity of the paste-aggregate environment, and the complications involved in measuring corrosion of polymer-coated reinforcing steel. Numerous problems remain to be solved in the practical application of electrochemical techniques to structures in the field, including reliable electrodes and contacts, electromagnetic interference and stray currents, choice of stable reference electrodes and the development of adequate equipment. In addition to the measurement problem itself, the choice of a measurement schedule that will provide a representative sampling of short and long term environmental conditions is another challenge that remains to be addressed.

SUMMARY

1) The discussion above has addressed some of the key issues in performing useful measurements of corrosion rates of corroding steel in concrete, by means of excitation-response electrochemical measurements. Simple linear polarization or potential step measurements would seem to be adequate to evaluate corrosion rates if the corroding system were to behave as a simple, discrete mixed potential electrode. However, current distribution effects coupled with the presence of a large reactive component of the interfacial impedance result in a highly convoluted polarization response of steel in concrete under many conditions. This situation tends to preclude the use of simple polarization measurements to evaluate corrosion rates of steel in concrete, unless some prior information on the impedance response of the system already exists to reveal the extent of complicating factors.

2) Corrosion rate evaluation by means of sophisticated methods of impedance measurement and analysis (such as in Ref.[44]) is conceptually possible. The implementation of these concepts is only now beginning to be attempted, and considerable experimental verification will be needed to establish the value of this approach. Knowledge of the actual polarization conditions present in steel in concrete (such as for example the extent of diffusional polarization, or the value of the interfacial capacitance) is necessary for the successful application of any measurement technique. This kind of information is not sufficiently available at present.

3) Methods based on excitation current confinement show promise in simplifying the system response so that only a restricted portion of steel is being examined. thus facilitating corrosion rate evaluation. At this time there is not enough information available to safely predict the extent of current confinement in each practical condition (for example, if more than one mat of reinforcing steel is present below the counter electrode). Additional development and verification will be necessary in this area.

BIBLIOGRAPHY

1. Anderson, K., Allard, B., Bengtsson, M. and Magnusson, B., Cement and Concrete Rsch., Vol. 19, p. 327, 1989.

2. Kayyali, O. et al, Cement and Concrete Rsch., Vol. 18, p.327, 1989.

3. Browne, R., "Mechanisms of Corrosion of Steel in Concrete in Relation to Design, Inspection and Repair of Offshore and Coastal structures", in Performance of Concrete in Marine Environment, Publication SP-65, American Concrete Institute, Detroit, 1980.

4. Monfore, G., "The Electrical Resistivity of Concrete", Journal of the PCA Research and Development Laboratories, May 1968, p.35.

5. Tuutti, K., Corrosion of Steel in Concrete, Swedish Cement and Concrete Research Institute, 1982.

6. O. Gjorv, O. Vennesland and A. El-Busaidy, Materials Performance, Vol.25, No.12, p.39 (1986).

7. Morehead, W., Diffusion of Dissolved Oxygen through Concrete (Discussion), Materials Performance, Vol.26, No.5, p.34, 1987.

8. Pickering, H., Corrosion, Vol.42, p.125, 1986.

9. Wyatt, B. and Irvine, D., Materials Performance, Vol. 26, p.12, December 1987.

10 Macdonald, D., "Transient Techniques in Electrochemistry, Plenum Publishing corporation, New York, 1977.

11. Shreir, L., Editor, Corrosion, Volume 1, Metal/Environment Reactions, Newnes-Butterworths, London, 1976.

12. Payne, R., Electroanal.Chem. and Interf. Electrochem., Vol. 41, p.277, 1973.

13. Schell, H. and Manning, D., Materials Performance, Vol. 24, p.18, July 1985.

14. Uhlig, H., and Revie, R., Corrosion and Corrosion Control, 3rd. Ed., John Wiley, New York, 1985.

15. Mansfeld, F.,"The Polarization Resistance Technique", in Advances in Corrosion Science and Technology, Vol. 6, M. Fontana and R. Staehle, Eds., Plenum Press, New York, 1976.

16. Andrade, C. and Gonzalez, J., Werkstoffe un Korrosion, Vol. 29, p.515, 1978.

17. S. Haruyama, "Faradic Impedance of Mixed Potential Electrode," Proc. Fifth Int. Cong. Metallic Corrosion, p.82, National Association of Corrosion Engineers, Houston (1974).

18. T. Tsuru, "Treatment of Diffusion Impedance in AC Impedance Method", 61st. Japan Soc. Corr. Eng. Symposium Report, pp.97-106 (1985).

19. A. A. Sagues, Corrosion Vol 44, 555 (1988).

20. D.Macdonald and M. McKubre "Electrochemical Impedance Techniques in Corrosion Science",in Electrochemical Corrosion Testing, p.110, ASTM STP 727, F. Mansfeld and U. Bertocci, Eds,. ASTM, Philadelphia (1981).

21 Epelboin, I., Gabrielly, C., Keddam, M. and Takenouti, H., "AC Impedance Applied to Corrosion Studies", in Electrochemical Corrosion Testing, p.150, ASTM STP 727, F. Mansfeld and U.Bertocci, Eds,. ASTM, Philadelphia (1981).

22. Kaesche, H., "Metallic Corrosion", NACE, Houston, 1985.

23. Andrade, C., Cruz Alonso, M. and Gonzalez, J., "An Initial Effort to Use the Corrosion Rate Measurements for Estimating rebar Durability", p.29 in Corrosion Rates of Steel in Concrete, ASTM STP 1065, N. Berke, V. Chaker and D. Whiting, Eds., ASTM, Philadelphia, 1990.

24. Clear, K. Measuring Rate of Corrosion of Steel in Field Concrete Structures, TRB 68th Annual Meeting, January 22-26, 1989, Paper Preprint No. 88-0324.

25. Escalante, E. and Ito, S., "Measuring the Rate of Corrosion of Steel in Concrete", p.86 in Corrosion Rates of Steel in Concrete, ASTM STP 1065, N. Berke, V. Chaker and D. Whiting, Eds., ASTM, Philadelphia, 1990.

26. Macdonald, D., J. Electrochem. Soc., Vol.,125, p.1443, 1978.

27. Shih, H., and Pickering, H., J. Electrochem. Soc., Vol 134, p.1943, 1987.

28. Shih, H., and Pickering, H., J. Electrochem. Soc., Vol. 134, p.1949, 1987.

29. Sagues, A., "Corrosion Measurements of Reinforcing Steel in Concrete Exposed to Various Aqueous Environments", Paper No. 118, Corrosion/87, National Association of Corrosion Engineers, Houston, 1987.

30. Gonzalez, J., Molina, A., Escudero, M. and Andrade, C., Corrosion Science, Vol 25, p. 519, 1985.

31. Gonzalez, J., Molina, A., Escudero, M. and Andrade, C., Corrosion Science, Vol 25, p. 917, 1985.

32. Sagues, A., Electrochemical Impedance of Corrosion Macrocells on Reinforcing Steel in Concrete, Paper No. 132, Corrosion/90, Nat. Assoc. of Corr. Engs., Houston, 1990.

33. Sagues, A. to be published.

34. D. Macdonald, M. McKubre and M. Urquidi-Macdonald, Corrosion, Vol.44, p.2 (1988).

35. J. R. Park and D. D. Macdonald, Corrosion Sci Vol 23, 295 (1983).

36. R. DeLevie, Electrochimica Acta, Vol.9, p.1231 (1964).

37. Keiser, H., Beccu, K., and Gutjahr, M., Electrochim. Acta, Vol.21, p.539, 1976.

38. Feliu, S., Gonzalez, J., Andrade, C. and Feliu, V., Materials and Structures, Vol. 22, p.199, 1989.

39. Feliu, S., Gonzalez, J., Andrade, C. and Feliu, V., Corrosion Science, Vol. 29, p.105, 1989.

40. Feliu, S., Gonzalez, J., Andrade, C. and Feliu, V., Corrosion, Vol. 44, p.761, 1988.

41. Urquidi-Macdonald, M., Rocha-Filho, R., El-Tantawy, Y., and Macdonald, D., "The Application of Electrochemical Impedance Spectroscopy for Calculating the Corrosion rate of Rebar in Reinforced Concrete", in SHRP Denver Workshop Proceedings, J. Broomfield and Il Jawed, Eds., Strategic Highway Research Program, Washington, 1990.

42. Lemoine, L., Wenger, F. and Galland, J., "Study of the Corrosion of Concrete Reinforcement by Electrochemical Impedance Measurement", p. 118 in Corrosion Rates of Steel in Concrete, ASTM STP 1065, N. Berke, V. Chaker and D. Whiting, Eds., ASTM, Philadelphia, 1990.

43. Elsener, B. and Bohni, H. "Potential Mapping and Corrosion of Steel in Concrete", p.143 in Corrosion Rates of Steel in Concrete, ASTM STP 1065, N. Berke, V. Chaker and D. Whiting, Eds., ASTM, Philadelphia, 1990.

44. Strategic Highway Research Program, Research Project ID008, Ultralow Frequency AC Impedance Spectroscopy, D.D. Macdonald, Principal Investigator. Washington, 1990.

45. Thompson, N., Lawson, K., and Beavers, J., Corrosion, Vol. 44, p.581, 1988.

46. R. Oltra and M. Keddam, Corrosion Sci. Vol.28, p.1 (1988).

47. Rammelt, U., and Reinhard, G., Corrosion Science, Vol.27, P.373, 1987.

48. Matthew Thomas, "Effect of Surface Roughness on the Double Layer Capacitance at The Steel/Alkaline Medium Interface", M.S. Thesis, University of South Florida (1988)

49. J. Dawson, "Corrosion Monitoring of Steel in Concrete", in Corrosion of Reinforcement in Concrete Construction, A.Crane, Ed., Ellis Horwood, Chichester (1983).

50. Zayed, A. and Sagues, A., Corrosion Science Vol.30, p.1025, 1990.

51. Matsuoka, K., Kihira, H., Ito, S., and Murata, T., "Corrosion Monitoring for Reinforcing Bars in Concrete", p. 103 in Corrosion Rates of Steel in Concrete, ASTM STP 1065, N. Berke, V. Chaker and D. Whiting, Eds., ASTM, Philadelphia, 1990.

52. Feliu, S.,Gonzalez, J., Escudero, M.,and Andrade, C., "Influence of Counter Electrode Size on the On-Site Measurement of Polarization Resistance in Concrete Structures", Paper No. 142, Corrosion/90, National Association of Corrosion Engineers, Houston, 1990.

53. John, D., Eden, D., Dawson, J. and Langford, P., "Corrosion Measurements of Reinforcing Steel and Monitoring of Concrete Structures", Paper No. 136, Corrosion/87, National Association of Corrosion Engineers, Houston, 1987.

54. Strategic Highway Research Program, Research Project C-101, Assessment of Physical Condition of Bridge Decks, P. Cady, Principal Investigator, Washington, 1990.

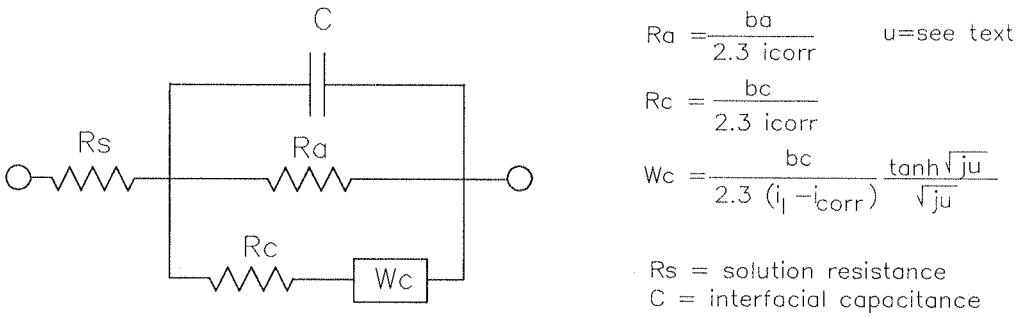

Figure 1 - Equivalent circuit of the interface of a discrete mixed-potential electrode with and activation-limited anodic reaction and a mixed activation/diffusion controlled cathodic reaction.

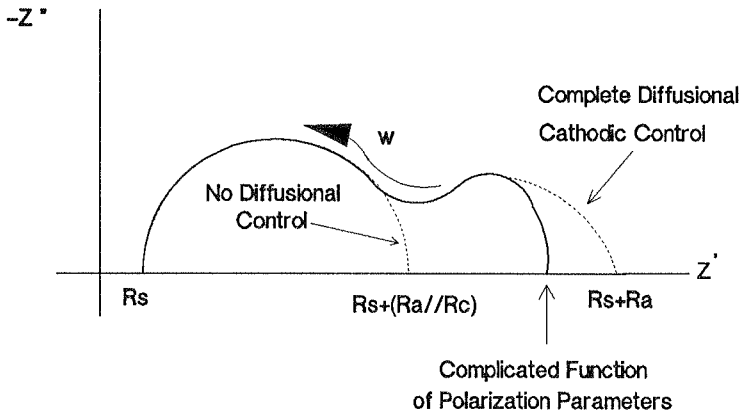

Figure 2 - Nyquist impedance diagram corresponding to the equivalent circuit shown in Figure 1. The solid line corresponds to mixed activation-diffusion control of the cathodic reaction. Dashed lines show the extreme diffusion cases and the corresponding values of the low-frequency impedance limit.

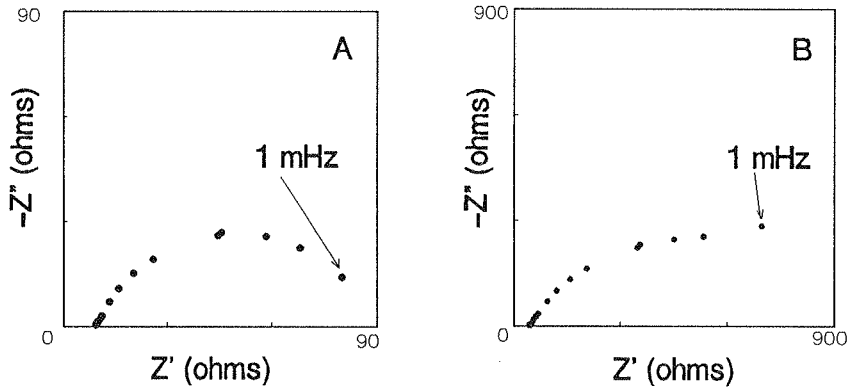

Figure 3 - Examples of typical EIS behavior of reinforced concrete beams undergoing active corrosion. In (A) the data tend to converge toward the real axis at the low frequency limit. In (B) the phase angle remains high at the lowest test frequencies.
A: 3 m-long beam, half of the length submerged in 15% NaCl solution.
B: 0.45 m-long column, lower 17.5 cm submerged in a 9000 ppm Cl^- solution [32].

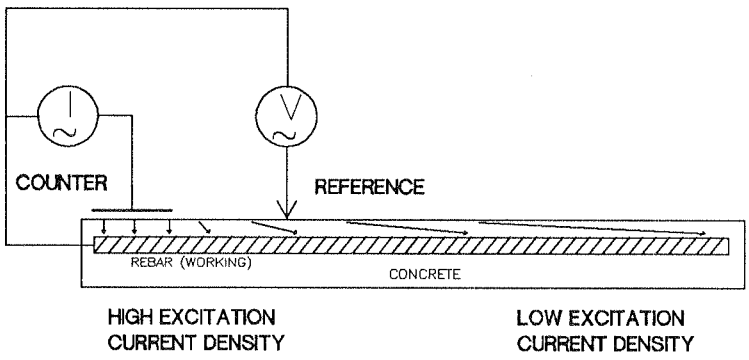

Figure 4 - Reinforced concrete beam excited near one end by an ac current source (I). Because of finite concrete conductivity, the excitation current density is highest near the counter electrode. Impedance calculations based on the measured ac voltage (V) and the excitation current will give different values along the beam.

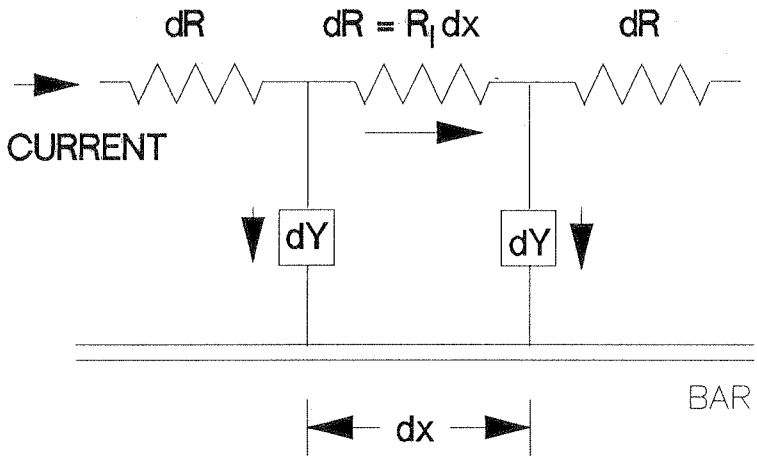

Figure 5 - Transmission-line model of a slender reinforced concrete beam [34, 38-40].

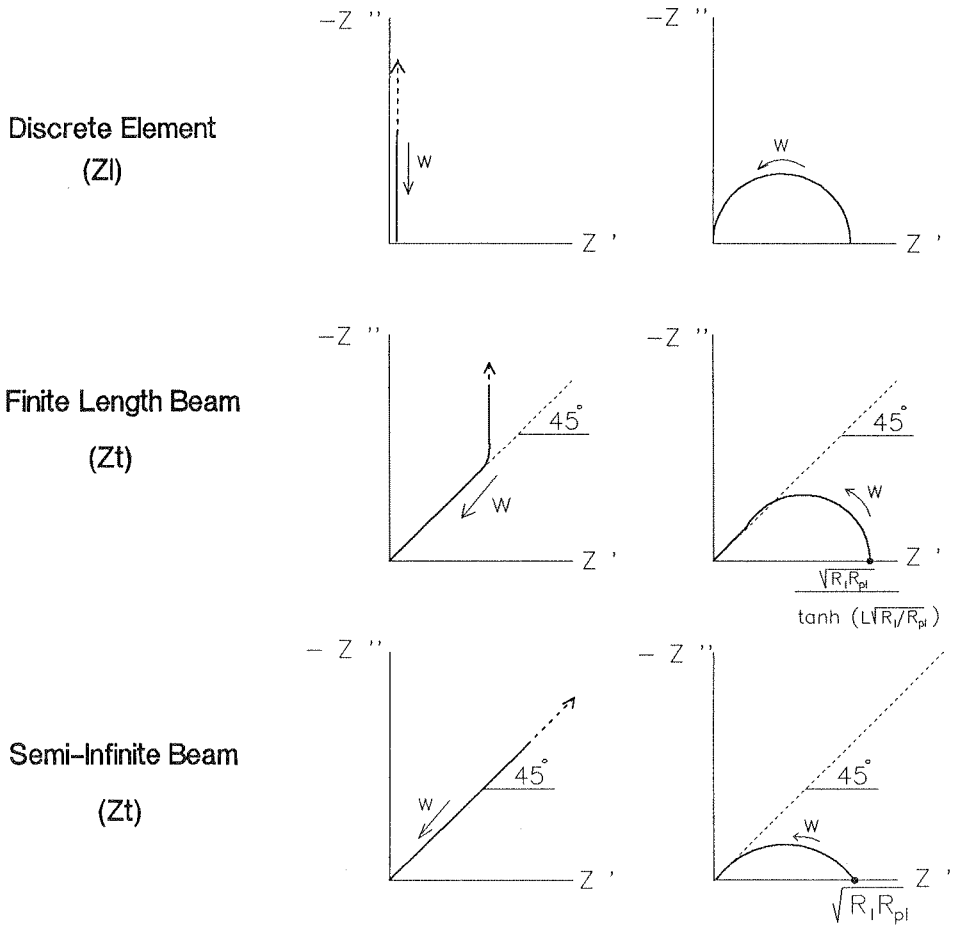

Figure 6. Impedance behavior expected for a discrete electrode (top diagram) and based on Eqs. (17) and (18) for a slender reinforced concrete beam excited at one end (center and bottom diagrams). The left side diagrams show the response in the absence of corrosion. The right side shows the response under uniform corrosion conditions, assuming that the impedance of each surface element corresponds to a simple polarization resistance-interfacial capacitance combination.

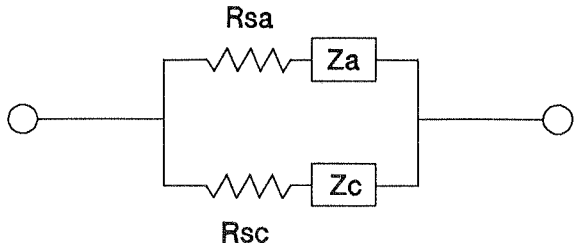

Figure 7. Simplified equivalent circuit of a reinforced concrete component containing a small localized anode and a larger cathode. Long-range current distribution effects (as in Figure 4) are not included here.

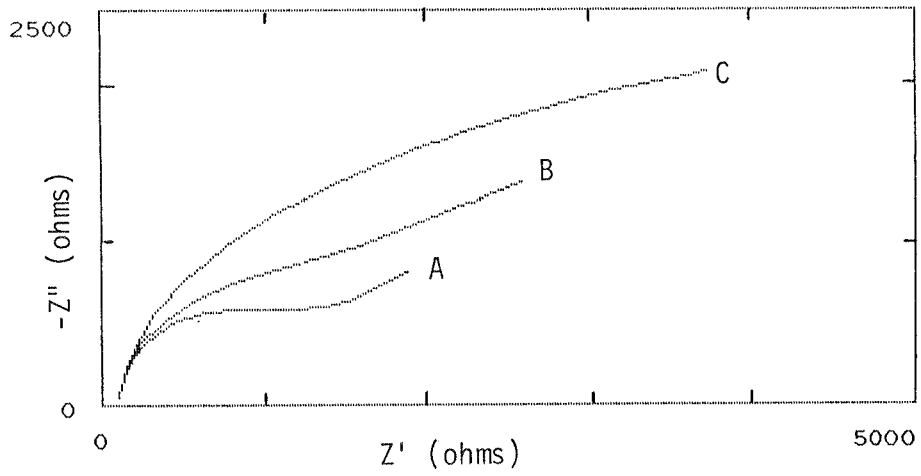

Figure 8. Calculated impedance response for circuit in Figure 7. The parameters are: anode area = 1 cm^2; Rsa=10,000 ohm; anodic current=63 uA; cathode area=100 anodic area; Rsc=Rsa/100. Impedances per Eqs. (15) and (16) (area-adjusted and w/capacitive component) with ba=60 mV; bc=160 mV; d=3cm; D=5 10^{-5} cm^2/sec; cathodic current-to-limiting current ratios of 0.98 (curve A); 0.99 (B) and 0.995 (C). Int.cap.=50uF/cm^2. Lowest frequency=1mHz.

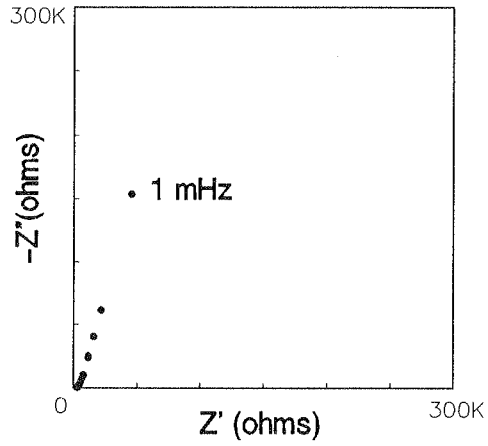

Figure 9. CPA behavior of sandblasted passive steel in concrete (from Ref.[32]). Rebar segment 5 cm long, 1 cm diameter in dry concrete.